

## Large-Scale Collective Properties of Self-Propelled Rods

Francesco Ginelli,<sup>1,2</sup> Fernando Peruani,<sup>1</sup> Markus Bär,<sup>3</sup> and Hugues Chaté<sup>1</sup>

<sup>1</sup>*Service de Physique de l'État Condensé, CEA-Saclay, 91191 Gif-sur-Yvette, France*

<sup>2</sup>*Institut des Systèmes Complexes de Paris Île-de-France, 57-59 rue Lhomond, 75005 Paris, France*

<sup>3</sup>*Physikalisch-Technische Bundesanstalt, Abbestrasse 2-12, 10587 Berlin, Germany*

(Received 6 November 2009; published 4 May 2010)

We study, in two space dimensions, the collective properties of constant-speed polar point particles interacting locally by nematic alignment in the presence of noise. This minimal approach to self-propelled rods allows one to deal with large numbers of particles, which exhibit a rich phenomenology distinctively different from all other known models for self-propelled particles. Extensive simulations reveal long-range nematic order, phase separation, and space-time chaos mediated by large-scale segregated structures.

DOI: [10.1103/PhysRevLett.104.184502](https://doi.org/10.1103/PhysRevLett.104.184502)

PACS numbers: 47.54.-r, 05.65.+b, 87.18.Gh, 87.18.Hf

Collective motion is a ubiquitous phenomenon observable at all scales, in natural systems [1] as well as human societies [2]. The mechanisms at its origin can be remarkably varied. For instance, they may involve the hydrodynamic interactions mediated by the fluid in which bacteria swim [3], the long-range chemical signaling driving the formation and organization of aggregation centers of *Dictyostelium discoideum* amoeba cells [4], or the local cannibalistic interactions between marching locusts [5]. In spite of this diversity, one may search for possible universal features of collective motion, a context in which the study of “minimal” models is a crucial step. Recently, the investigation of the simplest cases, where the problem is reduced to the competition between a local aligning interaction and some noise, has revealed a wealth of unexpected collective properties. For example, constant-speed, self-propelled, polar point particles with ferromagnetic interactions subjected to noise (as in the Vicsek model [6]) can form a collectively moving fluctuating phase with long-range polar order even in two spatial dimensions [7], with striking properties such as spontaneous segregation into ordered solitary bands moving in a sparse, disordered sea, or anomalous (“giant”) density fluctuations [8]. In contrast, active apolar particles with nematic interactions only exhibit quasi-long-range nematic order in two dimensions with segregation taking the form of a single, strongly fluctuating, dense structure with longitudinal order and even stronger density fluctuations than in the polar-ferromagnetic case [9,10].

Noting that these differences reflect those in the local symmetry of particles and their interactions, a third situation can be defined, intermediate between the polar-ferromagnetic model and the apolar nematic one, that of self-propelled polar particles aligning nematically. Such a mechanism is typically induced by volume exclusion interactions, when elongated particles colliding almost head-on slide past each other (Fig. 1). Thus, self-propelled polar point particles with apolar interactions can be conceived as

a minimal model for moving rods interacting by inelastic collisions [11–13]. Other relevant situations can be found in biology, such as gliding myxobacteria moving on a substrate [14], or microtubules driven by molecular motors grafted on a surface [15].

In this Letter, we study constant-speed polar point particles interacting locally by nematic alignment in the presence of noise. The simplicity of this model allows us to deal with large numbers of particles, revealing a phenomenology previously unseen in more complicated models sharing the same symmetries [11–13] but in agreement with the linear analysis of [16]. Our study, restricted to two space dimensions, shows, in particular, collective properties distinctively different from both those of the polar-ferromagnetic case and of active nematics: only nematic order arises in spite of the polar nature of the particles, but it seems genuinely long-ranged. Spontaneous density segregation is also observed, but here it appears as a bona fide phase separation: in the ordered side, a dense band occupying a fraction of space along which particles move in both directions arises when noise is strong enough. Its instability marks the order-disorder transition. It vanishes at strong noise, splitting the disordered phase in two. The class of polar particles aligning nematically exhibits thus a total of four phases.

Our model consists of  $N$  point particles moving off lattice at constant speed  $v_0$ . In two dimensions, particle  $j$  is defined by its (complex) position  $\mathbf{r}_j^t$  and orientation  $\theta_j^t$ , updated at discrete time steps according to

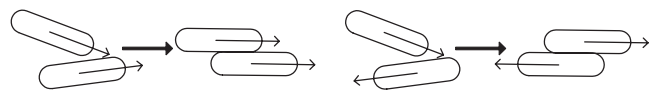


FIG. 1. Nematic alignment of polar particles illustrated by inelastic collisions of rods. Particles incoming at a small angle (left) align “polarly,” but those colliding almost head-on slide past each other, maintaining their nematic alignment (right).

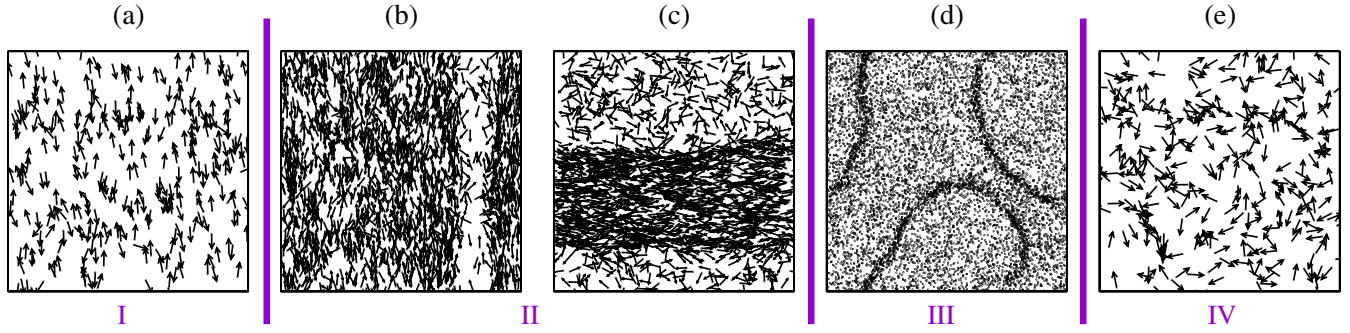


FIG. 2 (color online). (a)–(c) Typical steady-state snapshots at different noise values (linear size  $L = 2048$ ). (a)  $\eta = 0.08$ , (b)  $\eta = 0.10$ , (c)  $\eta = 0.13$ , (d)  $\eta = 0.168$ , (e)  $\eta = 0.20$ . Arrows indicate the polar orientation of particles [except in (d)]; only a fraction of the particles are shown for clarity reasons. For a movie corresponding to (d) see [19].

$$\theta_j^{t+1} = \arg \left[ \sum_{k \sim j} \text{sign}[\cos(\theta_k^t - \theta_j^t)] e^{i\theta_k^t} \right] + \eta \xi_j^t \quad (1)$$

$$\mathbf{r}_j^{t+1} = \mathbf{r}_j^t + v_0 e^{i\theta_k^{t+1}}, \quad (2)$$

where the sum is taken over all particles  $k$  within unit distance of  $j$  (including  $j$  itself), and  $\xi$  is a white noise uniformly distributed in  $[-\frac{\pi}{2}, \frac{\pi}{2}]$  [17]. (A continuous-time version of this model can be found in [18].) The system has two main control parameters: the noise amplitude  $\eta$ , and the particle density  $\rho = N/A$ , where  $A$  is the domain area. We consider periodic boundary conditions. Polar and nematic order can be characterized by means of the two time-dependent global scalar order parameters  $P(t) = |\langle \exp(i\theta_j^t) \rangle_j|$  (polar) and  $S(t) = |\langle \exp(i2\theta_j^t) \rangle_j|$  (nematic), as well as their asymptotic time averages  $P = \langle P(t) \rangle_t$  and  $S = \langle S(t) \rangle_t$ .

Here, we mostly report on the behavior of the system for  $\rho = \frac{1}{8}$  and  $v_0 = \frac{1}{2}$ , varying  $\eta$ . We start with a brief survey of the stationary states observed in a square domain of linear size  $L = 2048$  (Figs. 2 and 3). Despite the polar nature of the particles, only *nematic* orientational order arises at low noise, while  $P$  always remains near zero (not shown). This is in agreement with the findings of [16]. Both the ordered and the disordered regimes are subdivided in two phases, one that is spatially homogeneous [Figs. 2(a) and 2(e)], and one where density segregation occurs, leading to high-density ordered bands along which the particles move back and forth [Figs. 2(b)–2(d)]. A total of four phases is thus observed, labeled I to IV by increasing noise strength hereafter. Phases I and II are nematically ordered, phases III and IV are disordered.

Phase I, present at the lowest  $\eta$  values, is ordered and spatially homogeneous [Fig. 2(a)]. Nematic order arises quickly from any initial condition, even though long-lived dense polar packets are observed locally: statistically, two subpopulations of particles migrate in opposite directions [Fig. 4(a)], constantly exchanging particles. These “turn around” events occur at exponentially-distributed times  $\tau$  [Fig. 4(b)]. Increasing system size, the nematic order parameter  $S$  is almost constant, decaying slower than a power

law [Fig. 4(c)]. A good fit of this decay is given by an algebraic approach to a constant asymptotic value  $S^*$ . Thus, our data seem to indicate the existence of true long-range nematic order. (Quasi-long-range order, expected classically for two-dimensional nematic phases, is characterized by an algebraic decay of  $S$ .) A discussion of this striking fact is given below. Finally, as expected on general grounds for homogeneous ordered phases of active particles [10], phase I exhibits so-called giant number fluctuations: the fluctuations  $\Delta n^2 = \langle (n - \langle n \rangle)^2 \rangle$  of the average number of particles  $\langle n \rangle = \rho \ell^2$  contained in a square of linear size  $\ell$  follow the power law  $\Delta n \sim \langle n \rangle^\alpha$  with  $\alpha > \frac{1}{2}$  [Fig. 4(d)]. Our estimate of  $\alpha$  is compatible to that measured for *polarly* ordered phases  $\alpha = 0.8$  [8].

Phase II differs from phase I by the presence, in the steady state, of a low-density disordered region. In large-enough systems, for  $\eta \gtrsim \eta_{\text{I-II}} \simeq 0.098(2)$ , a narrow, low-density channel emerges rather suddenly, like in a nucleation process [Fig. 2(b)]. It becomes wider at larger  $\eta$  values, so that one can then speak of a high-density ordered band, typically oriented along one of the main axes of the box, amidst a disordered sea [Fig. 2(c)]. Particles travel along the high-density band, turning around or leaving the band from time to time. Within the band, nematic order with properties similar to those of phase I is found (slow decay of  $S$  with system size, giant number fluctuations).

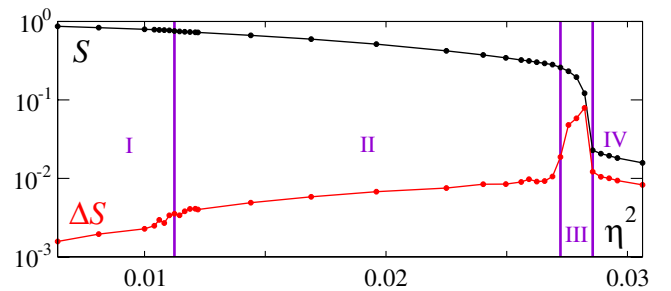


FIG. 3 (color online). Nematic order parameter  $S$  (in black) and its rms fluctuations  $\Delta S$  (in red) as function of the squared noise amplitude  $\eta^2$  for a square domain of linear size  $L = 2048$ . Here, and throughout the Letter, time averages are over at least  $10^6$  time steps.

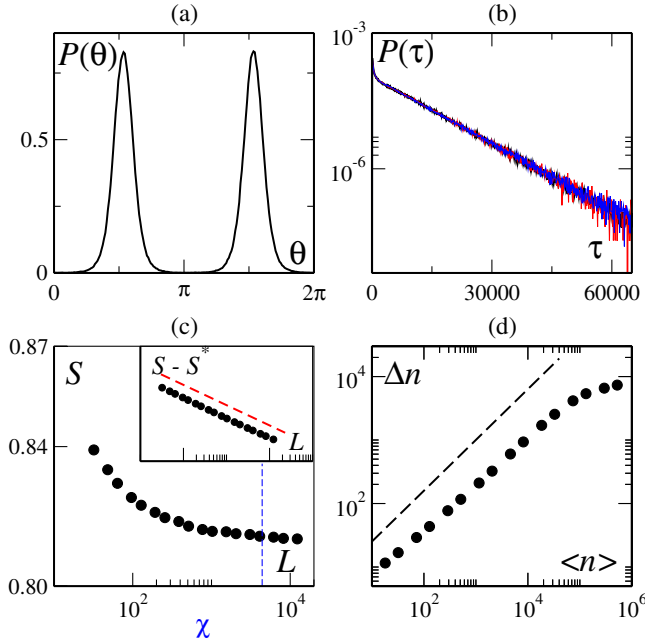


FIG. 4 (color online). Phase I (homogeneous nematic order,  $\eta = 0.095$ ). (a) Polar orientation probability distribution in a system of size  $L = 2048$ . (b) Distribution of particle transition times  $\tau$  between the two peaks of (a) for three different system sizes  $L = 512$ , 1024, and 2048 (black, red [light gray], and blue [dark gray] lines, respectively). (c) Nematic order parameter  $S$  vs system size  $L$  in square domains. The vertical dashed line marks the persistence length  $\chi \approx 4400$  (see text). Inset:  $S - S^* = 0.813063$  vs  $L$  (red dashed line:  $L^{-2/3}$  decay). (d) Number fluctuations  $\Delta n$  as a function of average particle number  $\langle n \rangle$  (see text) in a system of size  $L = 4096$  (dashed line: algebraic growth with exponent 0.8).

The (rescaled) band possesses a well-defined profile with sharper and sharper edges as  $L$  increases [Fig. 5(a)]. The fraction area  $\Omega$  occupied by the band is asymptotically independent of system size and decreases continuously as the noise strength  $\eta$  increases [Fig. 5(b)]. This, together with the nucleationlike process leading to the band, is suggestive of phase separation.

In phase III, spontaneous segregation into bands still occurs (for large-enough domains); however these thinner bands are unstable and constantly bend, break, reform, and merge, in an unending spectacular display of space-time chaos [Fig. 2(d)] [19]. Thus, the transition between phase II and III, located near  $\eta_{\text{II-III}} \approx 0.163(1)$ , is the order-disorder transition of the model. It resembles a long but finite wavelength instability of the band [see for instance Fig. 6(c)]. In this regime,  $S(t)$  fluctuates strongly (Fig. 3) and on very large time scales [Figs. 6(a)]. Nevertheless, these fluctuations behave normally [i.e., decrease like  $1/\sqrt{N}$ , Fig. 6(b)]. Thus, the space-time chaos self-averages, making phase III a bona fide disordered phase, albeit one with huge correlation lengths and times.

Increasing further the noise strength, the segregated bands vanish, leaving phase IV, an ordinary disordered

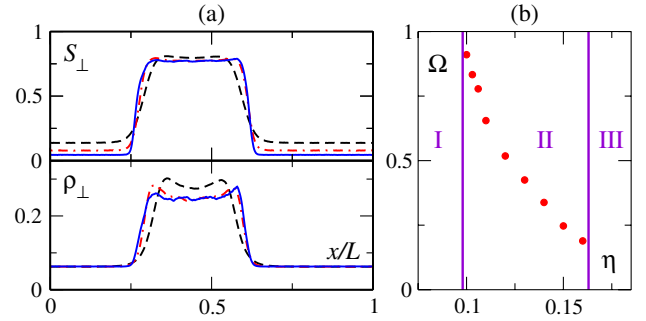


FIG. 5 (color online). Phase II (stable bands) (a) Rescaled transverse profiles in square domains of linear size  $L = 512$  (dashed black line), 1024 (dash-dotted red line), and 2048 (solid blue line) at  $\eta = 0.14$ . (Data averaged over the longitudinal direction and time, translated to be centered at the same location.) Bottom: density profiles. Top: nematic order parameter profiles. (b) Surface fraction  $\Omega$  as a function of  $\eta$  (defined here as the midheight width of the rescaled  $S$  profile).

phase, spatially homogeneous, and with very short correlations in space and time [Fig. 2(e)]. Near the transition point, at  $\eta_{\text{III-IV}} \approx 0.169(1)$ , the nematic order parameter  $S(t)$  exhibits bistability between a low amplitude, fast fluctuating state (typical of phase IV) and a larger amplitude, slowly fluctuating one typical of phase III (not shown). This suggests a discontinuous disorder-disorder transition between phase III and IV.

At this point, the most crucial question is perhaps that of the stability of the nematic order observed in phases I and II. Indeed, much of what we described above for large but finite systems relies on our conclusion of possible truly long-range (asymptotic) order [Fig. 4(c)]. On the one hand, one could argue that the exponential distributions of flight times between the two opposite polar orientations [Fig. 4(b)] define a finite persistence time  $\tau$  and a corresponding finite persistence length scale  $\chi \approx v_0\tau$  [indicated by the vertical dashed line in Fig. 4(c)]. Therefore, at scales much larger than  $\chi$ , the polar nature of our particles could become irrelevant, and the system would then behave like a fully nematic one, with only quasi-long-range order. As of now, we have been able to probe systems sizes up to 3 or 4 times the persistence length  $\chi$ . So far, as shown in Fig. 4(c), these systems comprising up to twenty million particles show no sign of breakdown of order. On the other hand,  $\chi$  is a single-particle quantity. Even though it is finite and system size independent, particles travel in rather dense polar packets which have flights longer than  $\chi$ . Indeed, the giant density fluctuations reported [Fig. 4(d)] indicate that denser, more ordered, and hence probably longer-lived packets occur in larger systems. But should this “polar packet lifetime” diverge with system size, then one would have a mechanism opening the door for the emergence of true long-range nematic order. To summarize this discussion, nematic order could break down for system sizes much larger than  $\chi$ , but our data [Figs. 4(c) and 4(d)] and the argument above suggest the

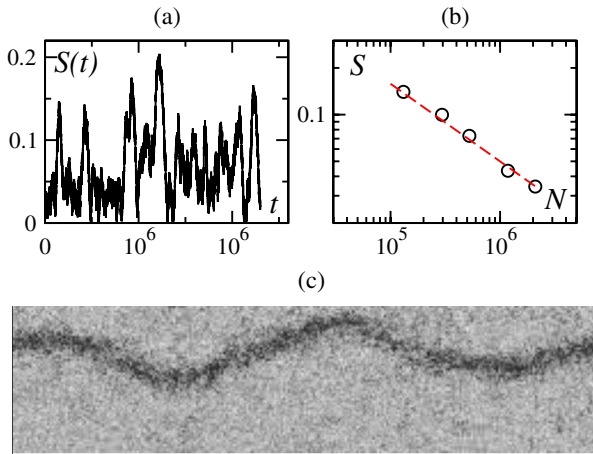


FIG. 6 (color online). Phase III (unstable bands,  $\eta = 0168$ ). (a) Typical nematic order parameter time series for a system of linear size  $L = 2048$ . (b)  $S$  vs  $N$  in square domains of increasing sizes. (The dashed line marks a  $1/\sqrt{N}$  decay.) (c) Snapshot of coarse-grained density field during the growth of the instability of an initially straight band in a  $2048 \times 512$  domain.

picture of two opposite polar components each with true long-range order (as in fully-polar models [20]) summing up to true nematic order.

Further work is needed, notably on the nature of the transitions between our phases, but most of our results are rather robust. Investigations at other densities than  $\rho = \frac{1}{8}$  show that the general picture presented holds, at least up to  $\rho = 1$  (not shown). Moreover, the introduction of soft-core repulsion between particles does *not* modify our main findings [21]. Thus, these are not due to the pointwise nature of the particles, and should also be observed in more detailed models of self-propelled rods if sufficiently large populations are considered.

Coming back to the approach of [16], our findings are in agreement with the linear instability found there of both the homogeneous nematically-ordered phase (our I-II transition), and of the homogeneous disordered phase (our IV-III transition). Further analytical work at the nonlinear level, possibly along the lines of [22], is needed, though, to account for the phenomenology found here.

We note also that our results, and in particular the space-time chaotic motion of the spontaneously segregated bands (phase III) [19], are reminiscent of the streaming and swirling regime which characterizes the aggregation of myxobacteria [14,23]. Our model suggests that no adhesion or chemical signaling is needed for such behavior to emerge. We therefore believe that our results may be relevant for the collective dynamics of gliding bacteria, biofilms and other cells with friction and moderate adhesion. The aspect of volume exclusion may also be an important ingredient in more complex models addressing animal groups or human crowds.

At a more general level, our findings reveal unexpected emergent behavior among even the simplest situations

giving rise to collective motion. Our model of self-propelled polar objects aligning nematically stands out as a member of a universality class distinct from both that of the Vicsek model [6–8] and of active nematics [9]. Thus, in this out-of-equilibrium context, the symmetries of the moving particles and of their interactions must be considered separately and are both relevant ingredients.

We thank J. Toner and S. Ramaswamy for fruitful discussions. This work was partially funded by the French ANR projects Morphoscale and Panurge, and the German DFG Grants No. DE842/2, No. SFB 555, and No. GRK 1558.

- [1] *Three Dimensional Animals Groups*, edited by J. K. Parrish and W. M. Hamner (Cambridge University Press, Cambridge, England, 1997), and references therein.
- [2] D. Helbing, I. Farkas, and T. Vicsek, *Nature (London)* **407**, 487 (2000).
- [3] A. Sokolov *et al.*, *Phys. Rev. Lett.* **98**, 158102 (2007).
- [4] E. Ben-Jacob *et al.*, *Adv. Phys.* **49**, 395 (2000).
- [5] P. Romanczuk, I. D. Couzin, and L. Schimansky-Geier, *Phys. Rev. Lett.* **102**, 010602 (2009).
- [6] T. Vicsek *et al.*, *Phys. Rev. Lett.* **75**, 1226 (1995).
- [7] J. Toner and Y. Tu, *Phys. Rev. Lett.* **75**, 4326 (1995); *Phys. Rev. E* **58**, 4828 (1998).
- [8] H. Chaté *et al.*, *Phys. Rev. E* **77**, 046113 (2008); G. Grégoire and H. Chaté, *Phys. Rev. Lett.* **92**, 025702 (2004).
- [9] H. Chaté, F. Ginelli, and R. Montagne, *Phys. Rev. Lett.* **96**, 180602 (2006).
- [10] S. Ramaswamy, R. A. Simha, and J. Toner, *Europhys. Lett.* **62**, 196 (2003); S. Mishra and S. Ramaswamy, *Phys. Rev. Lett.* **97**, 090602 (2006).
- [11] F. Peruani, A. Deutsch, and M. Bär, *Phys. Rev. E* **74**, 030904(R) (2006).
- [12] A. Kudrolli *et al.*, *Phys. Rev. Lett.* **100**, 058001 (2008).
- [13] H. H. Wensink and H. Löwen, *Phys. Rev. E* **78**, 031409 (2008).
- [14] L. Jelsbak and L. Sogaard-Andersen, *Proc. Natl. Acad. Sci. U.S.A.* **99**, 2032 (2002); D. Kaiser, *Nat. Rev. Microbiol.* **1**, 45 (2003).
- [15] F. Ziebert *et al.*, *Eur. Phys. J. E* **28**, 401 (2009).
- [16] A. Baskaran and M. C. Marchetti, *Phys. Rev. E* **77**, 011920 (2008); *Phys. Rev. Lett.* **101**, 268101 (2008).
- [17] Equation (1) is invariant under  $\theta_k^i \rightarrow \theta_k^i + \pi$  for any of the neighbors: the interaction has nematic symmetry.
- [18] F. Peruani, A. Deutsch, and M. Bär, *Eur. Phys. J. Special Topics* **157**, 111 (2008).
- [19] See supplementary material at <http://link.aps.org/supplemental/10.1103/PhysRevLett.104.184502> for a movie.
- [20] This is also suggested by the fact that the density fluctuations are governed by the same exponent as in the polar case [Fig. 4(d)], and by preliminary results showing phase ordering properties akin to those of the Vicsek model [21].
- [21] F. Peruani *et al.* (to be published).
- [22] E. Bertin, M. Droz, and G. Grégoire, *Phys. Rev. E* **74**, 022101 (2006); *J. Phys. A* **42**, 445001 (2009).
- [23] D. R. Zusman *et al.*, *Nat. Rev. Microbiol.* **5**, 862 (2007).